



## Comparative Analysis of Cellulose, Hemicellulose and Lignin on The Physical and Thermal Properties of Wood Sawdust for Bio-Composite Material Fillers

Cahyo Budiyantoro<sup>1</sup>, Ferriawan Yudhanto<sup>2\*</sup>

<sup>1</sup> Department of Mechanical Engineering, Universitas Muhammadiyah Yogyakarta 55183 Indonesia

<sup>2</sup> Department of Automotive Engineering Technology, Universitas Muhammadiyah Yogyakarta 55183 Indonesia

Corresponding Author Email: [ferriawan@umy.ac.id](mailto:ferriawan@umy.ac.id)

Copyright: ©2024 The authors. This article is published by IIETA and is licensed under the CC BY 4.0 license (<http://creativecommons.org/licenses/by/4.0/>).

<https://doi.org/10.18280/rcma.340114>

### ABSTRACT

**Received:** 9 November 2023

**Revised:** 4 December 2023

**Accepted:** 12 January 2024

**Available online:** 29 February 2024

#### Keywords:

*wood sawdust, hardwood, softwood, physical properties, thermal degradation*

This research compares the physical and thermal characteristics of three kinds of wood sawdust applied to bio-composites filler. Wood Sawdust of Sengon (softwood), Pine (softwood), and Teak (hardwood) have a crystalline structure (cellulose). The hydrochloric acid test found cellulose and other lignocellulosic content, such as hemicellulose and lignin. It contributed to the plant's strength. Adding a good filler in the polymer as a matrix with a high cellulose composition can increase the inter-mechanical bonding of bio-composites. Sengon sawdust has 48.98% cellulose content and contributes to the highest crystallinity index of 52.8%, calculated by the X-ray diffraction test. A high aspect ratio (L/D) on the bio-composite positively impacted the mechanical strength of bio-composite materials. The Scanning Electron Microscope (SEM) can show the morphology and calculate the aspect ratio of wood sawdust. Aspect ratio of wood sawdust from high to low i.e. Sengon (5.8), Pine (3.9), and Teak (1.5), respectively. Fourier transform infrared (FTIR) test to detect the twelve absorbance frequencies of the cellulose, hemicellulose, and lignin. Thermal degradation of all wood sawdust has the same initial degradation temperature ( $T_{onset}$ ) by 255°C and maximum degradation temperature ( $T_{max2}$ ) by 300°C.

## 1. INTRODUCTION

Wood is a natural source widely used as an alternative material for automotive body components, building construction, furniture, and home decoration. The various applied of each wood depend on anatomy, morphology, and chemical content, and it has different physical and mechanical properties of wood. Wood from tropical rainforest area generally has high of cellulose. The wood sawdust is waste of wood from carpenter industry. Therefore, It potential as a filler in bio-composite products. Natural resources to reinforcement of composite materials emphasize mechanical strength in hardness, tensile strength, flexural strength, and elastic modulus as fibre content properties [1, 2]. Other parameters, like aspect ratio and volume fraction, can improve load transfer on the interfacial layer to increase mechanical strength and have been widely studied [3, 4].

Hemicellulose, lignin, and many other substances have complex chemical chains. The main components, cellulose and lignin, are found in hardwood and softwood [5]. The kinds of hardwood are teak, maple, mahogany wood, etc. Softwood such as pine, sengon, spruce wood, etc. In recent years, wood sawdust has been used as a filler in thermoset and thermoplastic polymer composites. The wood species used as bio-composite products depend on physical, mechanical and thermal properties [6]. Furthermore, wood sawdust filler is an

additional material with a minor concentration in the thermoset resin such as unsaturated polyester, epoxy and phenolic given the excellent binding of the interfacial layers of laminated composite.

The Wood Plastic Composites (WPC) product aims to reduce environmental pollution and recycle industrial waste [7]. WPC materials were formed by wood sawdust fillers and thermoplastic polymers such as PP (polypropylene), PE (polyethylene), and PVC (polyvinylchloride) [8]. WPC has the advantage of being cheap, durable, and relatively low humidity. Furthermore, WPC from wood sawdust aims to reduce waste materials and air pollution.

Wood sawdust, used in the WPC composite materials, has irregular shapes and unequal sizes. Therefore, the shape is irregular, and the size has a large diameter of 700~800µm, coarse particles measuring 350~700µm, and fine particle size of 150~250µm. The size of these particles in making WPC affects density, porosity, and resistance to air absorption. Apart the size, the sawdust material's physical properties depend on the wood species [9, 10]. Hardwood cell walls, apart from cellulose and hemicellulose, also contain other components, namely guaiacyl and syringyl lignin, while softwood only contains syringyl lignin [11]. Lignin accounts for 20–35% of the dry weight of cell walls and provides wood with hardness, hydrophobicity and resistance bio-chemical on wood. Lignin is a hetero-polymer containing three main

chemical components: syringyl, guaiacyl, and p-hydroxyphenyl. The amount of lignin and the ratio of these units in the cell wall result from cell differences, which influence the chemical or physical properties of the cell wall. Therefore, the ability to predict cellulose and lignin distribution and unit ratios in woody plant cell walls is essential [12].

Adeniyi et al. [13] previously researched the effect of adding wood dust filler (*Isobertia Doka*) into a PS (polystyrene) matrix. The parameters studied were the weight fraction of the filler, namely 15, 30, and 45 wt.%, and the sawdust's size, 149, 250, and 841 $\mu$ m. The polymer used is polystyrene waste, used in the hand lay-up method and pressing on the mould. The results obtained for the tensile stress of adding 15 wt.% filler by 128MPa and increased when 30 wt.% filler was added, resulting in 550MPa and in addition, a concentration of 45 wt.%, tensile strength decreased significantly to 340MPa. Particle diameter is also a determining factor; the best results from varying powder sizes are 841 $\mu$ m. Adding wood filler at a concentration of 30 wt.% also increases the thermal resistance of the polystyrene/wood sawdust composite material, increasing from 1800 to 2262 J/Kg °C.

Uribe et al. [14] added micro cellulose from sugarcane bagasse material as a filler in laminate composites with glass fibre reinforcement. Making laminated composite and adding filler is done using vacuum-assisted infusion. The addition of this filler increases the mechanical strength of the interlayers. The filler fibrillates evenly along the glass fibres and forms an interfacial bond. The tensile strength and modulus of the layered composite increased from 230 to 260 Mpa and 13 to 15 Gpa, respectively. The impact of adding filler increases the flexural properties of laminated composite products. It increased flexural strength from 180 to 250Mpa and elastic modulus by 13 to 13.5Gpa.

Several previous research shows that wood sawdust has excellent potential to be used as an environmentally friendly filler for bio-composite materials. Physical parameters depend on the type of wood, which affects the mechanical properties of bio-composite materials. The physical and thermal characteristics of wood sawdust have never been studied before. Woody tropical rainforests in Indonesia are widely used for significant large industries, as well as for local industries and the bio-composite industry. This research aims to characterize three species of wood sawdust from equatorial rainforests in Indonesia before being applied as filler in WPC products. Wood sawdust fillers' properties are essential to Investigate.

## 2. MATERIAL AND METHOD

### 2.1 Chemical composition

Chemical composition test using the chlorite acid modification method. Holocellulose is a combined carbohydrate functional group chemical composition of cellulose and hemicellulose. The design of holocellulose is essential to know through a series of hydrochloric acid extraction processes. The holocellulose content varies depending on the type of wood sawdust. The wood sawdust was obtained from Gunung Kidul Village, Yogyakarta, Indonesia. The chemicals used in the chlorite acid method are toluene, ethanol, acetic acid, and chlorite sodium. Each wood

sawdust sample was extracted with ethanol and toluene (1:2 v/v) in soxhlet extractor for four times per hours along of 6 hours. Then, the sample used for analysis of the holocellulose and lignin content. The chemical composition measured procedure following the previous research by Liang et al. [15] which according the Chinese national standard of GB/T 2677.10-1995 for holocellulose and standard of GB/T 2677.8-1994 for Acid-insoluble lignin content to raw fibrous materials.

### 2.2 XRD test

X-ray diffraction is used to determine lattice parameter values, degree of crystallinity and crystal structure. The crystallinity index is a quantity that states the amount of crystal content in a material by comparing the area of the curve which is the area of the crystalline area with the total area of amorphous and crystalline. The instrument for the XRD (x-ray diffraction) test using a Shimadzu XRD-6000 operated at a voltage of 40kV, a current of 30mA, and the use of Cu K $\alpha$  radiation with a wavelength of 1.5406 Å. The scanning process range for cellulosic material was from 2 $\theta$  from 5° to 40° with an increment angle of 0.02° in 0.3 seconds or 0.60° counts per second (cps). XRD test aims to get the crystallinity index (CI) of raw wood sawdust. The CI in organic material can be determined by the Segal equation, as follows,

$$CI = (I_{002} - I_{amorph}) / I_{002}$$

where,  $I_{002}$  is the crystalline structure at  $2\theta=22-23^\circ$ , and  $I_{amorph}$  is the amorphous region at  $2\theta=18.8^\circ$ , based on JCPDS (Joint Committee on Powder Diffraction Standards).

### 2.3 FTIR test

Fourier transform infrared (FTIR) test using to investigates a functional group on woods sawdust through changes in intensity at a specific electromagnetic chemical bond and structure. Analysis for sample of FTIR spectrometer NICOLET iS10 type was made translucent to the infrared energy. The 2 mg wood sawdust material mixed with 50mg KBr (MERCK) and then pressed to became thin pellets. The thin pellet tested by range of resolution spectra from wavenumber 4000 $cm^{-1}$  to 400 $cm^{-1}$ .

### 2.4 Photo SEM

A scanning electron microscope (SEM) was used to observe the wood sawdust's morphology, which was investigated using the JEOL JCM-7000 type. The sawdust material is inserted into a circle jig to sputter the process with an electron beam thinly coated with platinum material (Pt) in the vacuum chamber using JEOL JEC-3000 FC. The platinum coating is needed for the conductivity of the organic sample. Vacuum 14.1Pa, sputtering voltage used 500V, current ten mA, deposition 10nm/min, grain size less than 5nm, temperature rise less than 10°C. It aims to clarify photos of the material surface. The JEOL JCM-7000 was set at 5kV to obtain the desired image with a magnification range of 50 and 250 times. Different magnifications are needed to calculate the aspect ratio (L/D) and detailed morphology observation.

### 2.5 TGA/DTG test

The most crucial aspect of TGA operation is the validity of

measurements made. Confidence in data collection can be achieved through regular calibration; mass and temperature calibrations must be performed. The calculation of the Curie point of the standard performs temperature calibrations. The thermal stability of wood sawdust using a Shimadzu TGA-50 tool. It was carried out every 20°C/min temperature increase with a flow rate of 50ml.min<sup>-1</sup> from temperature at 30°C to 500°C, using Nitrogen gas (N<sub>2</sub>). The TGA (Thermogravimetric Analysis) curve is a function of temperature (°C) and weight loss (%). A differential thermogravimetry curve (DTG) is generated as the first derivative of the weight concerning temperature or time. The DTG curve could be used to provide both qualitative and quantitative information about the sample. It showing endothermic and exothermic reactions. An endothermic reaction means absorbing heat, and an exothermic reaction means releasing heat.

### 3. RESULTS AND DISCUSSION

#### 3.1 Chemical composition analysis

Composition test using the hydrochloric acid method to extract fiber, primarily to obtain the holocellulose and alpha cellulose (I $\alpha$ ) content. I $\alpha$  is the main element that forms plant cell walls-glucose polymer with  $\beta$ -1,4 glucoside chemical bonds in straight chains. The basic form of glucose is cellobiose [16, 17]. Long cellulose chains are connected via hydrogen bonds and van der Waals forces [18]. The results of composition tests on three different types of wood showed that the high cellulose content was for Sengon wood at 48.98%, then pine at 45.68%, and Teak wood with the lowest cellulose value, namely 41.33%. The different results slightly by Kaida et al. [19], Wiyono et al. [20], and Rizanti et al. [21] were founded the chemical composition cellulose of Sengon, Pine and Teak wood 52.5%, 54.9% and 48.8%, respectively. Chemical composition test results could be seen on Table 1.

The lignin content supports and binds cellulose and hemicellulose in plant cell walls so plants can stand firmly. Lignin is a heterogeneous compound consisting of the elements carbon (C), hydrogen (H), and oxygen (O). In contrast to cellulose, which is formed from carbohydrate groups, lignin is formed from an arrangement of aromatic groups linked to each other by aliphatic chains [22, 23]. The carbonyl content is very dominant in the aromatic group. The lignin composition is predominant in wood plants, even Teak wood, by 33.43% (hardwood). It is higher than Sengon and Pinewood by 26.66% and 26.37%, respectively.

**Table 1.** Chemical composition of three kinds of wood Sawdust

Woods Sawdust	$\alpha$ -Cellulose (%)	Lignin (%)	Hemicellulose (%)
Sengon	48.98	26.66	23.33
Pine	45.68	26.37	24.99
Teak	41.33	33.43	24.45

Another component wood is hemicellulose. This polysaccharide is easily dissolved in alkaline solutions. Hemicellulose consists of D-glucose, D-Galactose, D-mannose, D-xylose, and L-arabinose units [24, 25]. The hemicellulose content in the three types of wood is almost the same, by 23.33, 24.99 and 24.45% for Sengon, Pine, and Teak wood, respectively. Sengon has the most minor hemicellulose

content compared to the two types of wood. The composition results show that Sengon and Pine wood sawdust have the most potential to be used as a composite filler because the cellulose content higher than Teak wood.

#### 3.2 Crystallinity analysis

Cellulose consists of both amorphous and crystalline regions. Hemicellulose and lignin are amorphous (non-crystalline). The crystallinity of wood sawdust could be calculated with the Segal equation based on the XRD spectra graph. The Figure 1 shows the XRD spectra graph with two visible peaks at  $2\theta=15.8^\circ$  (111) and  $2\theta=22.6^\circ$  (002), which that the presence of crystal plane (111) and (002), indicates cellulose in wood structured [26]. These peaks represent the lattice plane for the wood's crystalline structure type I (I $\alpha$  and I $\beta$ ) cellulose. Alpha cellulose (I $\alpha$ ) is the most common form in nature, dominating the chemical component of wood. In contrast, the amorphous structure shows the valley at  $2\theta=18.8^\circ$ . Beta cellulose is an amorphous material like lignin and hemicellulose. The amorphous regions in the raw Sengon, Pine, and Teak wood have more than 35% content. The crystallinity index (CI) of natural wood for Sengon, Pine, and Teak wood are shown in Table 2. The Sengon wood sawdust has a higher CI (52.8%) than the others, confirming their chemical composition with high alpha cellulose content. The density of wood sawdust of Sengon (0.4-0.75gr/cm<sup>3</sup>) and Pine wood (0.77-0.86gr/cm<sup>3</sup>) is lower than Teak wood (0.60-1.16gr/cm<sup>3</sup>) [27].

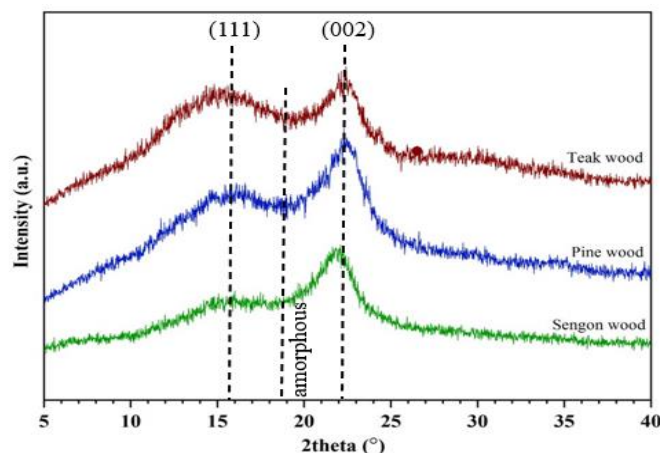


**Figure 1.** XRD curve of three kinds wood sawdust

**Table 2.** Crystallinity index of woods sawdust

Materials	I <sub>002</sub> (cps)	I <sub>amor</sub> (cps)	CI (%)
Teak Wood	629	384	38.95
Pine Wood	756	419	44.57
Sengon Wood	483	228	52.80

#### 3.3 IR spectrum analysis

FTIR (Fourier Transform Infrared) identifies and quantifies specific functional groups. A change in the characteristic pattern of absorption bands in the FTIR curve indicates a difference in the chemical composition of the lignocellulosic materials. Main bands of infrared spectrum shown in Table 3. It divides three wavenumber regions: short IR (<400 cm<sup>-1</sup>), mid-IR (400-4000cm<sup>-1</sup>), and near IR (4000-13000cm<sup>-1</sup>) of the three types, the most widely used is the mid-IR spectrum,

including in analyzing organic materials. Mid-IR is classified into four wavenumber regions [28], namely:

- (i) 2500-4000 $\text{cm}^{-1}$  there is single bond region (O-H, N-H, C-H)
- (ii) 2000-2500 $\text{cm}^{-1}$  there is triple bond region ( $\text{C}\equiv\text{N}$ ,  $\text{C}\equiv\text{C}$ )
- (iii) 1500-2000 $\text{cm}^{-1}$  there is double bond band region ( $\text{C}=\text{O}$ ,  $\text{C}=\text{C}$ ,  $\text{C}=\text{N}$ )
- (iv) 600-1500 $\text{cm}^{-1}$  there is finger print region

**Table 3.** Main bands of infrared spectrum of woods sawdust

Wavenumber ( $\text{cm}^{-1}$ )	Band Assignment
3410	O-H stretching of hydrogen-bond
2924	C-H stretching, Alkynes
2370	$\text{C}\equiv\text{N}$ stretching, Nitriles
2115	$\text{C}\equiv\text{C}$ stretching, Alkynes
1736	syringyl and guaiacyl ring plus $\text{C}=\text{O}$
1650	$\text{C}=\text{O}$ stretching vibration inconjugated carbonyl of lignin
1506	Aromatic skeletal vibrations
1425	C-C stretching, Aromatic
1240	S-syringyl ring and C-O stretching in lignin and xylan
1130	S-syringyl ring and C-O stretching in G-lignin (hard wood)
1054	C-O stretching vibration (cellulose and hemicellulose)
895	Stretching in Pyranose ring

Figure 2 shows that two peaks appeared on the range absorbance between 4000-2500, there are 3410 $\text{cm}^{-1}$ , and 2924 $\text{cm}^{-1}$  shows the O-H stretching and H-bonded identified to alcohols and phenols groups and symmetric and asymmetric stretching C-H vibration shows acetyl groups [29-31]. The absorbance on peak 1736 $\text{cm}^{-1}$  with  $\text{C}=\text{O}$  stretching usually assigned identified aldehydes, ester and aliphatic hydrocarbon shows characteristics of the guaiacyl lignin type seen prominent on the hardwood and rather than on softwoods [32].

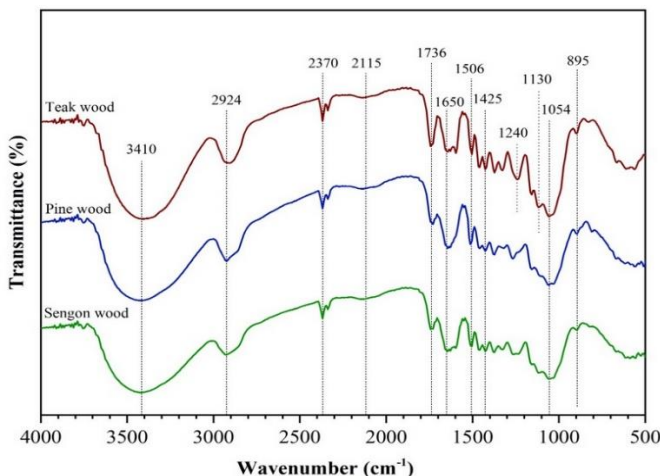


**Figure 2.** FTIR spectra of three kinds of wood sawdust

The syringyl and guaiacyl lignin units exist on the wavenumber of 1736 $\text{cm}^{-1}$  is attributed to phenol esterification and the alcohol of the propanoic chain ( $\text{C}\alpha$  and  $\text{C}\gamma$ ) [33, 34]. Wavenumbers of 1650 $\text{cm}^{-1}$  and 1506 $\text{cm}^{-1}$  indicate the presence of  $\text{C}=\text{O}$  stretching vibration and C-O aromatic

skeletal vibration groups, which are identical to the presence of amorphous material (lignin and hemicellulose) [35-37]. According to Pandey [38] this both frequencies are a part of the aromatic aryl compound on the  $\text{C}=\text{C}$  aromatic ring stretch. This element is found in hardwood and softwood. The ranges 1750-1500 $\text{cm}^{-1}$  a peak appearance absorbance at 1650 $\text{cm}^{-1}$  shows  $\text{C}=\text{C}$  stretching vibration identified carbonyl compound group [39, 40].

A sharp and dominant peak was found at 1240 $\text{cm}^{-1}$ , which shows C-O stretching, which indicates a higher amount of S-Syringyl and xylan which is usually found on hardwood than softwood. G-lignin and S-syringyl are shown at wave number 1130 $\text{cm}^{-1}$ , which only belongs to the hardwood species. Wavenumber 1054 $\text{cm}^{-1}$  indicates secondary alcohol, which identifies the presence of cellulose and hemicellulose, while wavenumber 895 $\text{cm}^{-1}$  indicates ring glucose groups [40].

### 3.4 SEM image analysis

The aspect ratio of Teak wood sawdust is the smallest compared to the other two wood species. The aspect ratio (L/D) is the critical length of wood sawdust as a discontinuous fibre. The high aspect ratio influences the increase in the mechanical strength of the bio-composite material. The high aspect ratio impacts the inter-mechanical bonding filler and matrix.

Figure 3 shows the failure schematic type of discontinuous fibers on the matrix of bio-composite material, including cracking and debonding. The illustrated filler phenomena by tensile test on the bio-composite specimen tensile test like on. The high amorphous material (lignin) causing the appearance of voids in the matrix. It impacted debonding failure. Neither than high cellulose content (high CI) causes excellent inter-mechanical bonding between filler and matrix, and it impacted crack in the matrix.

Figure 4 shows SEM images with magnifications of 50 and 250 times, and is measured by Image-J software to calculated diameter and length of wood sawdust. The morphology of Teak sawdust has a larger grain size with an average diameter of 180.5 $\mu\text{m}$  (D) and a height of 267.9 $\mu\text{m}$  (L). This distribution shows an aspect ratio (L/D) value of 1.5 (Figure 4 (a)).

The morphology of Pine wood sawdust is more heterogeneous than that of Teak wood sawdust in size (Figure 4 (b)). It can be observed from the image of the distribution of diameter and length have high deviation. The aspect ratio of Pine wood sawdust is 3.8. It was obtained by measuring the diameter and length of Pine wood sawdust by 115.3 $\mu\text{m}$  (D) and 437.7 (L)  $\mu\text{m}$ . The highest aspect ratio showed that Sengon's diameter by 57.4 $\mu\text{m}$  (D) and length is 333.2 $\mu\text{m}$  (L) (Figure 4 (c)). It shows aspect ratio is 5.8, it indicates that Sengon wood sawdust has potential as a filler bio-composite materials. The distribution diameter and length of three kinds wood sawdust are shown in Figure 5.

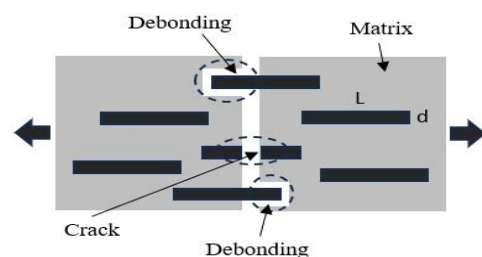


**Figure 3.** Schematic discontinuous fiber of failures type

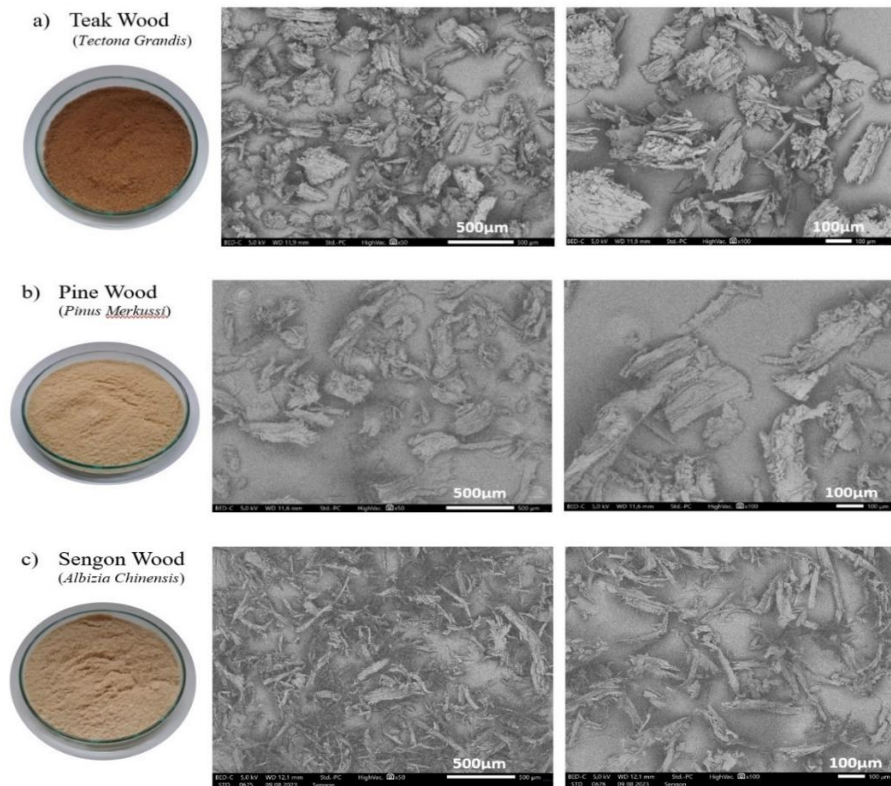


Figure 4. The morphology of diameter (D) and length (L) of three kinds of wood sawdust

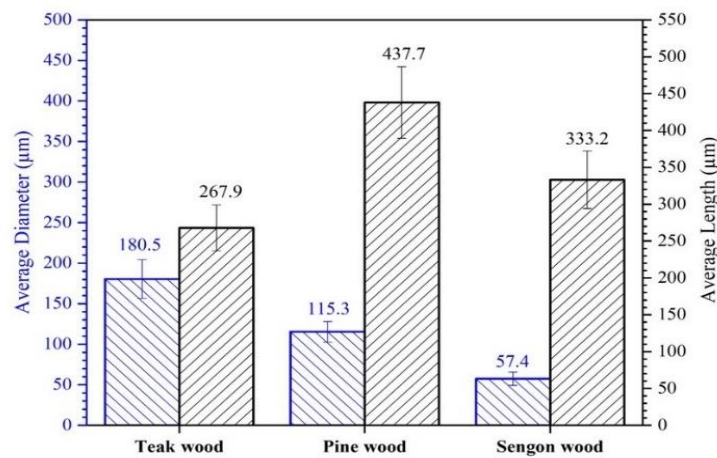


Figure 5. The distribution of diameter (D) and length (L) of three kinds wood sawdust

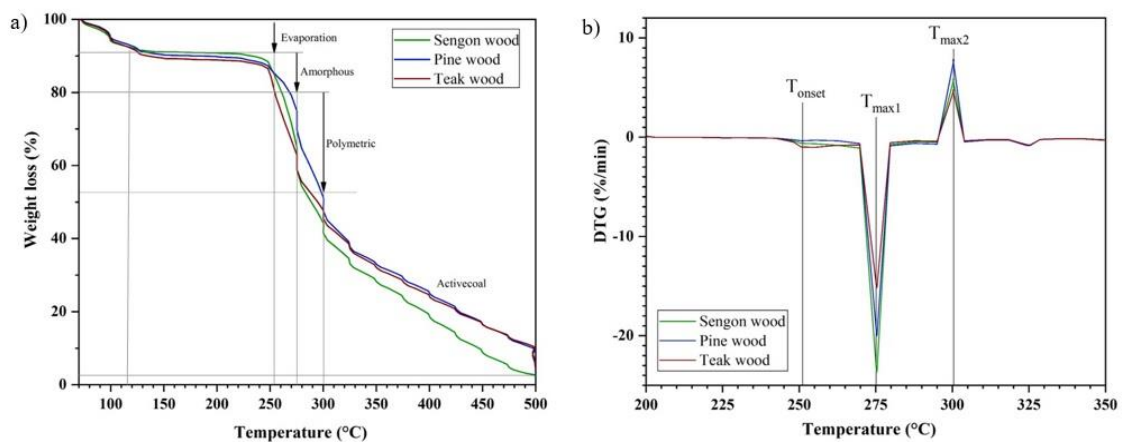


Figure 6. Three kinds wood sawdust thermal degradation: a) TGA and b) DTG curve

### 3.5 TGA/DTG analysis

Thermal stability of sawdust material tested by TGA (Thermogravimetric Analysis) equipment. The results produce a curve graph of the relationship between weight loss (%) and temperature (Figure 6(a)). The numerical derivative of TGA is DTG (Derivative Thermogravimetry), which helps to determine the occurrence of the initial ( $T_{onset}$ ) and maximum degradation temperature ( $T_{max}$ ) of the materials. Apart from that, it also helps to see the endothermic and exothermic reactions that occur by DTG curve (Figure 6(b)). The appearance of a decrease in the weight of the starting material of 9-10 wt.% at an initial temperature of 120-255°C, the presence of water vapor, and other extractive substances contained in lignocellulosic materials such as wood sawdust.

Hemicellulose (amorphous material) degrades at 275°C until it experiences a weight loss of 20 wt.%. Lignin has longer and stronger polymer chains, so it is more heat-resistant and begins to degrade at 300°C until it experiences a weight loss of 47 wt.%. Meanwhile, cellulose begins to break down after 300 to 500°C, and leaving a 2-10 wt.% residue. This is similar to Gao et al. [41] research on pine sawdust in that hemicellulose was degraded in the temperature range of 225-350°C. Meanwhile, other amorphous substances, such as lignin, are degraded at 250-500°C. Cellulose has high crystallinity and it is only degraded in the 325-350°C range. Heat resistance research by Pedreño-Rojas et al. [22] on Pine wood sawdust obtained  $T_{max}$  at a temperature of 359.45°C. Chen and Chen [16] investigate the thermal resistance of biomass (cellulose, hemicellulose, and lignin) by TGA test. The rapid decomposition is hemicellulose at the lowest temperature (223-250°C).

Cellulose takes place at high temperatures 326-369°C, in contrast the lignin decomposed over cellulose there is a temperature range 311-461°C [34, 42]. The results of thermal tests in this research on the three kind woods are Teak, Pine, and Sengon wood sawdust got the best thermal resistance. Teak wood sawdust, whereas the negligible heat absorption (Endothermic) at  $T_{max1}$  with a value of 15%.min<sup>-1</sup>, then the Pine wood sawdust value by 20%.min<sup>-1</sup>. and the most outstanding value for Sengon wood value by 28%.min<sup>-1</sup> It shows that Sengon sawdust is not resistant to high temperatures. Meanwhile, the temperature resistance of Pine is between Teak and Sengon wood sawdust. The  $T_{max2}$  is decomposed lignin and cellulose at temperature 300°C. The heat release (exothermic) at  $T_{max2}$ , indicated Sengon easy release heat, and then Teak wood is difficult to release heat.

**Table 4.** Thermal degradation of other wood species

Wood Species	$T_{onset}$ (°C)	$T_{max1}$ (°C)	$T_{max2}$ (°C)	Residue at 500°C (%)	Ref.
<i>Quercus alba</i>	258	322	385	12	[43]
<i>Pinus radiata</i>	219	-	388	14	[43]
<i>Eucalyptus grandis</i>	245	321	387	13	[43]
<i>Acacia cyclops</i>	235	325	385	13	[43]
Pine wood ( <i>Pinus merkussi</i> )	255	275	300	11	This study
Teak wood ( <i>Tectona grandis</i> )	255	275	300	11	This study
Sengon wood ( <i>Albizia chinensis</i> )	255	275	300	2	This study

The Table 4 is the previous research compares the thermal stability between different woods species and this study.  $T_{onset}$  is onset temperature, at which degradation start and  $T_{max1}$  and  $T_{max2}$  are decomposition temperature there are appear as the sharp peak on the DTG graph. The high  $T_{max2}$  indicated the high amount of amorphous material especially lignin bond the cellulose. Furthermore, the highly branched molecular structure makes hydroxyl groups in the lignin chemical structure difficult to modify, and then resulting in poor bonding properties for bio-composite. It causes alot of voids in the bio-composite materials and impact low mechanical strength. So, the thermal stability became increase along with increases the crystallinity of cellulose.

### 4. CONCLUSION

The physical characteristics of the three kinds of wood sawdust (Teak, Pine, and Sengon) show that Sengon has a high crystallinity of 52.8% (48.98% cellulose content) and a high aspect ratio of 5.8, which are two essential factors as a filler as a reinforcement of bio-composites. The thermal degradation of all three types of wood sawdust has the same initial degradation ( $T_{onset}$ ) at 255°C and maximum temperature ( $T_{max2}$ ) at 300°C. Teak wood is good for thermal stability but has a low crystallinity index, aspect ratio, and low amount of cellulose. Teak wood sawdust shows a large amount of amorphous content; to eliminate the amorphous materials, they could be soaked in an alkali solution at a specific concentration to improve the crystallinity index.

### ACKNOWLEDGMENT

This research was funded by the *Direktorat Riset, Teknologi, dan Pengabdian kepada Masyarakat* (DRTPM) of the Ministry of Research, Technology and Higher Education, Indonesia, based on Contract No: 0536/E5/PG.02.00/2023

### REFERENCES

- [1] Najafi, S.K., Hamidinia, E., Tajvidi, M. (2006). Mechanical properties of composites from sawdust and recycled plastics. *Journal of Applied Polymer Science*, 100(5): 3641-3645. <https://doi.org/10.1002/app.23159>
- [2] Chindaprasirt, P., Hiziroglu, S., Waisurasingha, C., Kasemsiri, P. (2015). Properties of wood flour/expanded polystyrene waste composites modified with diammonium phosphate flame retardant. *Polymer Composites*, 36(4): 604-612. <https://doi.org/10.1002/pc.22977>
- [3] Eskander, S.B., Tawfik, M.E. (2019). Impacts of gamma irradiation on the properties of hardwood composite based on rice straw and recycled polystyrene foam wastes. *Polymer Composites*, 40(6): 2284-2291. <https://doi.org/10.1002/pc.25036>
- [4] Teacă, C.A., Shahzad, A., Duceac, I.A., Tanasă, F. (2023). The re-/up-cycling of wood waste in wood-polymer composites (wpcs) for common applications. *Polymers*, 15(16): 3467. <https://doi.org/10.3390/polym15163467>
- [5] Salih, S.A., Kzar, A.M. (2015). Studying the utility of using reed and sawdust as waste materials to produce

- cementitious building units. *Journal of Engineering*, 21(10): 36-54.
- [6] Selke, S.E., Wichman, I. (2004). Wood fiber/polyolefin composites. *Composites Part A: Applied Science and Manufacturing*, 35(3): 321-326. <https://doi.org/10.1016/j.compositesa.2003.09.010>
- [7] Vallittu, P.K. (2015). High-aspect ratio fillers: Fiber-reinforced composites and their anisotropic properties. *Dental Materials*, 31(1): 1-7. <https://doi.org/10.1016/j.dental.2014.07.009>
- [8] Chan, C.M., Vandi, L.J., Pratt, S., Halley, P., Richardson, D., Werker, A., Laycock, B. (2018). Composites of wood and biodegradable thermoplastics: A review. *Polymer Reviews*, 58(3): 444-494. <https://doi.org/10.1080/15583724.2017.1380039>
- [9] Rizki, M., Tamai, Y., Koda, K., Kojima, Y., Terazawa, M. (2010). Wood density variations of tropical wood species: Implications to the physical properties of sawdust as substrate for mushroom cultivation. *Wood Research Journal*, 1(1): 34-39.
- [10] Martins, C.I., Gil, V., Rocha, S. (2022). Thermal, mechanical, morphological and aesthetical properties of rotational molding pe/pine wood sawdust composites. *Polymers*, 14(1): 193. <https://doi.org/10.3390/polym14010193>
- [11] Huang, Y., Wang, L., Chao, Y., Nawawi, D.S., Akiyama, T., Yokoyama, T., Matsumoto, Y. (2012). Analysis of lignin aromatic structure in wood based on the IR spectrum. *Journal of Wood Chemistry and Technology*, 32(4): 294-303. <https://doi.org/10.1080/02773813.2012.666316>
- [12] Yamashita, D., Kimura, S., Wada, M., Takabe, K. (2016). Improved Mäule color reaction provides more detailed information on syringyl lignin distribution in hardwood. *Journal of Wood Science*, 62(2): 131-137. <https://doi.org/10.1007/s10086-016-1536-9>
- [13] Adeniyi, A.G., Abdulkareem, S.A., Adeoye, S.A., Ighalo, J.O. (2022). Preparation and properties of wood dust (isoberlinia doka) reinforced polystyrene composites. *Polymer Bulletin*, 79(6): 4361-4379. <https://doi.org/10.1007/s00289-021-03718-6>
- [14] Uribe, B.E.B., Chiromito, E.M.S., Carvalho, A.J.F., Tarpani, J.R. (2017). Low-cost, environmentally friendly route for producing CFRP laminates with microfibrillated cellulose interphase. *Express Polymer Letters*, 11(1). <https://doi.org/10.3144/expresspolymlett.2017.6>
- [15] Liang, L., Wei, L., Fang, G., Xu, F., Deng, Y., Shen, K., Tian, Q., Wu, T., Zhu, B. (2020). Prediction of holocellulose and lignin content of pulp wood feedstock using near infrared spectroscopy and variable selection. *Spectrochimica Acta Part A: Molecular and Biomolecular Spectroscopy*, 225: 117515. <https://doi.org/10.1016/j.saa.2019.117515>
- [16] Chen, H., Chen, H. (2014). Chemical composition and structure of natural lignocellulose. *Biotechnology of Lignocellulose: Theory and Practice*, 25-71. [https://doi.org/10.1007/978-94-007-6898-7\\_2](https://doi.org/10.1007/978-94-007-6898-7_2)
- [17] Yudhanto, F., Jamasri, J., Rochardjo, H.S.B. (2018). Physical and thermal properties of cellulose nanofibers (CNF) extracted from Agave cantala fibers using chemical-ultrasonic treatment. *International Review of Mechanical Engineering (IREME)*, 12(7): 597. <https://doi.org/10.15866/ireme.v12i7.14931>
- [18] Chami Khazraji, A., Robert, S. (2013). Interaction effects between cellulose and water in nanocrystalline and amorphous regions: A novel approach using molecular modeling. *Journal of Nanomaterials*, 2013: 1-10. <https://doi.org/10.1155/2013/409676>
- [19] Kaida, R., Kaku, T., Baba, K.I., Oyadomari, M., Watanabe, T., Hartati, S., Sudarmonowati, E., Hayashi, T. (2009). Enzymatic saccharification and ethanol production of Acacia mangium and Paraserianthes falcataria wood, and elaeis guineensis trunk. *Journal of Wood Science*, 55: 381-386. <https://doi.org/10.1007/s10086-009-1038-0>
- [20] Wiyono, B., Tachibana, S., Tinambunan, D. (2006). Chemical composition of indonesian pinus merkusii turpentine oils, gum oleoresins and rosins from sumatra and java. *Pakistan Journal of Biological Sciences*, 9(1): 7-14. <https://doi.org/10.3923/pjbs.2006.7.14>
- [21] Rizanti, D.E., Darmawan, W., George, B., Merlin, A., Dumarcay, S., Chapuis, H., Gérardin, C., Gelhay, E., Raharivelomanana, P., Sari, R.K., Syafii, W., Mohamed, R., Gerardin, P. (2018). Comparison of teak wood properties according to forest management: Short versus long rotation. *Annals of Forest Science*, 75(2): 1-12. <https://doi.org/10.1007/s13595-018-0716-8>
- [22] Pedreño-Rojas, M.A., Morales-Conde, M.J., Rubio-de-Hita, P., Pérez-Gálvez, F. (2019). Impact of wetting-drying cycles on the mechanical properties and microstructure of wood waste-gypsum composites. *Materials*, 12(11): 1829. <https://doi.org/10.3390/ma12111829>
- [23] Collard, F.X., Blin, J. (2014). A review on pyrolysis of biomass constituents: Mechanisms and composition of the products obtained from the conversion of cellulose, hemicelluloses and lignin. *Renewable and Sustainable Energy Reviews*, 38: 594-608. <https://doi.org/10.1016/j.rser.2014.06.013>
- [24] Yuan, T.Q., Xu, F., He, J., Sun, R.C. (2010). Structural and physico-chemical characterization of hemicelluloses from ultrasound-assisted extractions of partially delignified fast-growing poplar wood through organic solvent and alkaline solutions. *Biotechnology Advances*, 28(5): 583-593. <https://doi.org/10.1016/j.biotechadv.2010.05.016>
- [25] Yue, Z., Sun, L.L., Sun, S.N., Cao, X.F., Wen, J.L., Zhu, M.Q. (2022). Structure of corn bran hemicelluloses isolated with aqueous ethanol solutions and their potential to produce furfural. *Carbohydrate Polymers*, 288: 119420. <https://doi.org/10.1016/j.carbpol.2022.119420>
- [26] Jaouadi, M. (2021). Characterization of activated carbon, wood sawdust and their application for boron adsorption from water. *International Wood Products Journal*, 12(1): 22-33. <https://doi.org/10.1080/20426445.2020.1785605>
- [27] Martha, R., Mubarak, M., Darmawan, W., Syafii, W., Dumarcay, S., Charbonnier, C.G., Gerardin, P. (2021). Biomolecules of interest present in the main industrial wood species used in indonesia-a review. *J. Renew. Mater*, 9: 399-449. <http://dx.doi.org/10.32604/jrm.2021.014286>
- [28] Nandiyanto, A.B.D., Oktiani, R., Ragadhita, R. (2019). How to read and interpret FTIR spectroscopy of organic material. *Indonesian Journal of Science and Technology*, 4(1): 97-118. <https://doi.org/10.17509/ijost.v4i1.15806>

- [29] Yudha, V., Yudhanto, F., Rochardjo, H.S.B., Hariyanto, S.D. (2021). Cellulose microfibrils from salacca midrib fiber isolated by the mechanical treatment. *Jurnal Selulosa*, 11(01): 1-8. <http://dx.doi.org/10.25269/jssel.v11i01.319>
- [30] Yudhanto, F., Yudha, V., Jamasri, J., Wisnujati, A. (2022). Effect of alkali soaking time on physical and morphological properties of Agave cantala fiber. In *AIP Conference Proceedings*. AIP Publishing, Yogyakarta, Indonesia, 2499(1). <https://doi.org/10.1063/5.0104998>
- [31] HAMIDU, L.A.J., AROKE, U.O., JOCK, A.A. (2023). Physicomechanical properties of optimized particleboard produced from softwood sawdust and rice husk.
- [32] Fatkhurohman, F., Rochardjo, H.S.B., Kusumaatmaja, A., Yudhanto, F. (2020). Extraction and effect of vibration duration in ultrasonic process of cellulose nanocrystal (CNC) from ramie fiber. In *AIP Conference Proceedings*. AIP Publishing, 2262(1). <https://doi.org/10.1063/5.0015794>
- [33] Tang, W., Xu, J., Fan, Q., Li, W., Zhou, H., Liu, T., Guo, C., Ou, R., Hao X., Wang, Q. (2022). Rheological behavior and mechanical properties of ultra-high-filled wood fiber/polypropylene composites using waste wood sawdust and recycled polypropylene as raw materials. *Construction and Building Materials*, 351: 128977. <https://doi.org/10.1016/j.conbuildmat.2022.128977>
- [34] Lourenço, A., Pereira, H. (2018). Compositional variability of lignin in biomass. *Lignin-Trends and Applications*, 65-98.
- [35] Ilyas, R.A., Sapuan, S.M., Ishak, M.R. (2018). Isolation and characterization of nanocrystalline cellulose from sugar palm fibres (*Arenga Pinnata*). *Carbohydrate Polymers*, 181: 1038-1051. <https://doi.org/10.1016/j.carbpol.2017.11.045>
- [36] Shamskar, K.R., Heidari, H., Rashidi, A. (2016). Preparation and evaluation of nanocrystalline cellulose aerogels from raw cotton and cotton stalk. *Industrial Crops and Products*, 93: 203-211. <https://doi.org/10.1016/j.indcrop.2016.01.044>
- [37] Selvan, M.T., Jenish, I., Ramesh, M., Sahayaraj, A.F. (2023). Characterization of *Plumeria pudica* bark fiber for reinforcing lightweight polymer composites and evaluating its physical, chemical, and thermal properties. *Biomass Conversion and Biorefinery*, 1-14. <https://doi.org/10.1007/s13399-023-05172-y>
- [38] Pandey, K.K. (1999). A study of chemical structure of soft and hardwood and wood polymers by FTIR spectroscopy. *Journal of Applied Polymer Science*, 71(12): 1969-1975. [https://doi.org/10.1002/\(SICI\)1097-4628\(19990321\)71:12%3C1969::AID-APP6%3E3.0.CO;2-D](https://doi.org/10.1002/(SICI)1097-4628(19990321)71:12%3C1969::AID-APP6%3E3.0.CO;2-D)
- [39] Zoia, L., Salanti, A., Giorgione, C., Gentili, R., Citterio, S., Gandolfi, I., Franzetti, A., Orlandi, M. (2021). Integrated biological and chemical characterisation of a pair of leonardesque canal lock gates. *Plos One*, 16(3): e0247478. <https://doi.org/10.1371/journal.pone.0247478>
- [40] Esteves, B., Velez Marques, A., Domingos, I., Pereira, H. (2013). Chemical changes of heat treated pine and eucalypt wood monitored by FTIR. *Maderas. Ciencia Y Tecnología*, 15(2): 245-258. <http://dx.doi.org/10.4067/S0718-221X2013005000020>
- [41] Gao, N., Li, A., Quan, C., Du, L., Duan, Y. (2013). TG-FTIR and Py-GC/MS analysis on pyrolysis and combustion of pine sawdust. *Journal of Analytical and Applied Pyrolysis*, 100: 26-32. <https://doi.org/10.1016/j.jaap.2012.11.009>
- [42] Chen, D., Cen, K., Zhuang, X., Gan, Z., Zhou, J., Zhang, Y., Zhang, H. (2022). Insight into biomass pyrolysis mechanism based on cellulose, hemicellulose, and lignin: Evolution of volatiles and kinetics, elucidation of reaction pathways, and characterization of gas, biochar and bio-oil. *Combustion and Flame*, 242: 112142. <https://doi.org/10.1016/j.combustflame.2022.112142>
- [43] Shebani, A.N., Van Reenen, A.J., Meincken, M. (2008). The effect of wood extractives on the thermal stability of different wood species. *Thermochimica Acta*, 471(1-2): 43-50. <https://doi.org/10.1016/j.tca.2008.02.020>

## NOMENCLATURE

Å	Angstrom
$I_{002}$	Maximum intensity (crystalline region)
$I_{\text{amor}}$	Minimum intensity (amorphous region)
CI	Crystallinity Index
kV	Kilo Volt
cps	Counts per second
wt.%	Weigh percentage
$T_o$	Temperature onset/initial degradation
$T_{\text{max}}$	Temperature maximum degradation

## Greek symbols

$I_\alpha$	Alpha cellulose
$I_\beta$	Beta cellulose
$2\theta$	Angle between transmitted and reflected beam